Coronary Flow Assessment Using 3-Dimensional Ultrafast Ultrasound Localization Microscopy

Oscar Demeulenaere, Zulma Sandoval, Philippe Mateo, Alexandre Dizeux, Olivier Villemain, Romain Gallet, Bijan Ghaleh, Thomas Deffieux, Charlie Deméné, Mickael Tanter, et al.

Coronary flow assessment by 3D ultrafast ultrasound localization microscopy

Brief title: coronary microcirculation assessment by ultrasound

Oscar Demeulenaere[1], MS, Zulma Sandoval[1], PhD, Philippe Mateo[1], MS, Alexandre Dizeux[1], PhD, Olivier Villemain[1], MD, PhD, Romain Gallet[2], MD, PhD, Bijan Ghaleh[2], PhD, Thomas Deffieux[1], PhD, Charlie Demené[1], PhD, Mickael Tanter[1], PhD, Clément Papadacci[1], PhD, and Mathieu Pernot[1], PhD

[1]Physics for Medicine, ESPCI, INSERM U1273, CNRS UMR 8063, PSL University, Paris

[2]Inserm U955-IMRB, Equipe 03, UPEC, Ecole Nationale Vétérinaire d'Alfort, Maisons-Alfort, France

Corresponding address: mathieu.pernot@inserm.fr

Physics for Medicine, ESPCI

17 rue Moreau, 75012 Paris, France

Tel: +33686821309

Relationship with industry: Nothing to disclose

Funding support: This study was supported by the European Research Council under the European Union's Seventh Framework Program (FP/2007-2013) / ERC Grant Agreement n°

311025 and by the Fondation Bettencourt-Schueller under the program "Physics for Medicine".

Acknowledgements

This study was supported by the European Research Council under the European Union's Seventh Framework Program (FP/2007-2013) / ERC Grant Agreement n° 311025 and by the Fondation Bettencourt-Schueller under the program "Physics for Medicine". We acknowledge the ART (Technological Research Accelerator) biomedical ultrasound program of INSERM. The authors thank Lotfi Slimani for the support with µCT acquisitions and fruitful discussions.

Author contributions

M.P., C.P. and P.M conceived the study. O.D., C.P., and M.P. developed sequence acquisitions, O.D., P.M., O.V., C.P. and M.P. acquired data. O.D., Z.S., C.P., T.D., C.D., A.D., M.T and M.P. performed data processing. O.D., Z.S., C.P, M.T. and M.P. interpreted the results. M.P, C.P., and O.D. wrote the first draft of the manuscript with substantial contribution from A.D, Z.S, O.V and P.M. All authors edited and approved the final version of the manuscript.

Abstract

Objective: To demonstrate three-dimensional coronary ultrasound localization microscopy (CorULM) of the whole heart beyond the acoustic diffraction limit (<20 μm resolution) at ultrafast frame rate (>1000 images/s).

Background: Direct assessment of the coronary microcirculation has long been hampered by the limited spatial and temporal resolutions of cardiac imaging modalities.

Methods: CorULM was performed in isolated beating rat hearts (N=6) with ultrasound contrast agents (Sonovue, Bracco), using an ultrasonic matrix transducer connected to a high channel-count ultrafast electronics. We assessed the 3D coronary microvascular anatomy, flow velocity and flow rate of beating hearts under normal conditions, during vasodilator adenosine infusion and coronary occlusion. The coronary vasculature was compared to μCT performed on the fixed heart. *In vivo* transthoracic CorULM was eventually assessed on anaesthetized rats (N=3).

Results: CorULM enables the tri-dimensional visualization of the coronary vasculature in beating hearts at a scale down to microvascular structures (<20 μm resolution). Absolute flow velocity estimates range from 10mm/s in tiny arterioles up to more than 300 mm/s in large arteries. Fitting to a power law, the flow rate-radius relationship provides an exponent of 2.61 (r^2=0.96, p<0.001) which is consistent with theoretical predictions and experimental validations of scaling laws in vascular trees. A two-fold increase of the microvascular coronary flow rate is found in response to adenosine which is in good agreement with the overall perfusion flow rate measured in the aorta (control measurement) that increased from 8.80 ± 1.03 mL/min to 16.54 ± 2.35 mL/min (p<0.001). The feasibility of CorULM was demonstrated *in vivo* for N=3 rats

Conclusion: CorULM provides unprecedented insights into the anatomy and function of coronary arteries at the microvasculature level in beating hearts. This new technology is

highly translational and has the potential to become a major tool for the clinical investigation of the coronary microcirculation.

Key words: Ultrasound, imaging, coronary, blood flow, microcirculation, volumetric imaging, microscopy

Abbreviations:

2D 2-dimensional

3D 3-dimensional

CFR Coronary Flow Reserve

CMD Coronary Microcirculation Disease

CorULM Coronary Ultrasound Localization Microscopy

ECG electrocardiogram

IQ in-phase and quadrature

LAD Left Anterior Descending

LV Left Ventricle

LVP Left Ventricular Pressure

MB Micro-Bubbles

MI Myocardial Infarction

PRF Pulse Repetition Frequency

RF Radio-Frequency

SVD Singular Value Decomposition

µCT Micro Computed Tomography

ULM Ultrasound Localization Microscopy

Introduction

Coronary microcirculation (i.e coronary flow in vessels smaller than 300µm) plays a key role in the control of cardiac perfusion[1]. Patients with Coronary Microvascular Disease (CMD) have poor prognosis with significantly higher rates of cardiovascular events, including hospitalization for heart failure, sudden cardiac death, and myocardial infarction (MI)[1]. Likewise, microvascular obstruction following reperfusion of a myocardial infarction, a phenomenon so called no-reflow, is the most relevant predictor of adverse outcome.

Up to date, although anatomy of the large vessels can be easily assessed, only functional assessments of the coronary microcirculation are available either through imaging (PET[2], CMR[3] and contrast echocardiography[4]) or through invasive measurements[5]. These exams can provide hemodynamic information such as Myocardial Blood Flow (MBF) and Coronary Flow Reserve (CFR) in response to the vasodilator adenosine. However, there is currently no available tool to image directly the entire coronary microcirculation in clinical or preclinical settings, which in turn has limited considerably the knowledge on the coronary microcirculation pathophysiology and the development of effective therapeutic strategies. Indeed, direct visualization of the full coronary architecture including complex microvascular network remains out of reach of current cardiac imaging modalities mainly because of the low spatial and temporal resolutions or sensitivity limitations[6]. The association of anatomic and hemodynamic exploration at the microscopic scale could allow a better understanding of the adaptation of the coronary microcirculation to physiological conditions (aging, exercise) or to pathophysiological stresses (proximal artery stenosis, O2 consumption/perfusion imbalance). Moreover, besides contrast echocardiography, none of the exams evaluating microcirculation can be easily repeated because of their availability, the risk of irradiation, and the risk of complications for invasive assessment. Consequently, we are currently lacking of a technique that would allow repeated anatomical and functional evaluation of the

coronary microcirculation in order to determine the mechanisms of the functional alterations but also to address the effect of the different treatments.

Recently, ultrafast ultrasound broke the conventional ultrasound resolution barrier via localization of single circulating microbubbles (MB) in the blood flow[7]. Ultrafast Ultrasound Localization Microscopy (ULM) allowed mapping microvascular flows at high spatial resolution (~10µm), an order of magnitude smaller than the ultrasound diffraction limit, and at depths much greater than the traditionally frequency-limited imaging depth[8]. However, coronary network arrangement is complex and arbitrarily oriented in all three dimensions which greatly limit two dimensional ULM assessed in cross-sections. Furthermore, deformation of the heart as well as large and rapid out-of-plane motion induced by physiological events, mostly cardiac and respiratory motions, create significant errors in localization[9] and cannot be efficiently corrected without a three dimensional approach.

Here, we overcome these issues and demonstrate coronary ultrasound localization microscopy (CorULM) for direct visualization and quantification of the coronary microvascular flows in beating perfused rat hearts. Our approach relies on volumetric ultrafast imaging with an ultrasonic matrix transducer connected to a high channel-count ultrafast electronics[10]. 3D-ULM is then used to track the microbubble circulation and quantify the flow velocity in the entire coronary vasculature[11]. A multiscale 3D motion correction is applied on the localization center over a few tens of cardiac cycles which enabled to reconstruct the 3D coronary microvascular anatomy, flow velocity and flow rate of beating hearts under normal conditions, during vasodilator adenosine infusion and coronary occlusion. Finally, we demonstrate the *in vivo* feasibility of CorULM on closed chest animals.

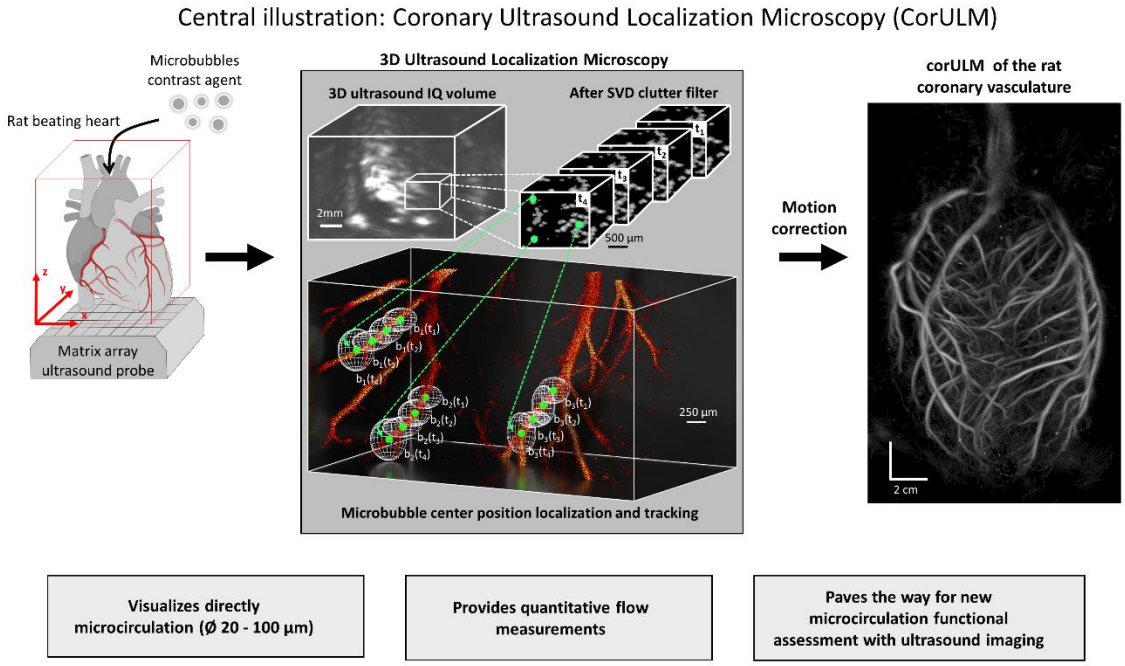

Central Illustration: **Coronary Ultrasound Localization Microscopy (CorULM).** CorULM relies on the injection of microbubbles contrast agents into the coronary vasculature and 3D ultrafast ultrasound imaging with a matrix array pobe. Thanks to its high volume rate, this imaging modality allows the detection of microbubbles center position and tracking over time. After correction of cardiac contraction and breath motion, CorULM provides tri-dimensional superresolved images of the anatomy and flow velocity of the coronary vasculature in beating hearts at a scale down to microvascular structures (<20 µm resolution). CorULM provides also insights into function of coronary arteries at the microvasculature level. This new technology is highly translational and has the potential to become a major tool for the clinical investigation of the coronary microcirculation.

Methods

Langendorff isolated perfused heart – Experimental model

The Sprague Dawley male rats (189±18 g, N=6) were anesthetized by intraperitoneal injection of Ketamine (80mg/kg) and Xylasine (10mg/kg). The heart was quickly removed and placed in oxygenated Krebs-Henseleit solution. The aorta was cannulated and perfused by the Langendorff method with oxygenated Krebs-Henseleit solution at constant pressure at the beginning (50 mmHg, temperature 37±0.2°C)[12]. A latex water-filled balloon was inserted into the left ventricular chamber and connected to a pressure transducer for continuous measurement of isovolumic left ventricular pressure (LVP), heart rate, end-diastolic pressure,

left ventricular developed pressure. Coronary pressure and flow were measured and monitored by an isolated heart system (Emka Technologies). All the recorded parameters were computed by a dedicated data acquisition and analysis software (Labchart, ADInstruments). LVP signal was used to trig synchronized ultrasound acquisitions. The hearts were electrically stimulated at 350 bpm via two silver wires; one on the right atria, one on the left ventricle connected to a Function Generator (Tektronix).

Isolated hearts were perfused by Krebs-Henseleit solution for normal beating activity at 60 and 120 mmHg coronary pressure. Coronary vasodilation was obtained by adding adenosine at 10^{-5} mmol/L under a constant pressure of 120mmHg. A perfusion system (perfused isolated heart system, Emka Technologies, Paris, France) was used to control the perfusion pressure and flow rate. In constant pressure mode, the device automatically adapted the coronary flow by changing the peristaltic perfusion pump velocity. The perfusion flow was computed from the pump velocity after calibration. Cardiac arrest was obtained by decreasing temperature of solution containing the heart and perfusion solution from 37°C to 4°C. Contrast agent (Sonovue, Bracco) at 0.33% dilution was added in the perfused solution.

Occlusion of the Left Anterior Descending (LAD) artery was performed by ligating the artery at the basal-mid level of the left ventricle. In this experiment, the flow rate was maintained constant and the perfusion pressure was automatically adapted by the flow system.

Figure 1. 3D CorULM principles

a) Set-up and acquisition

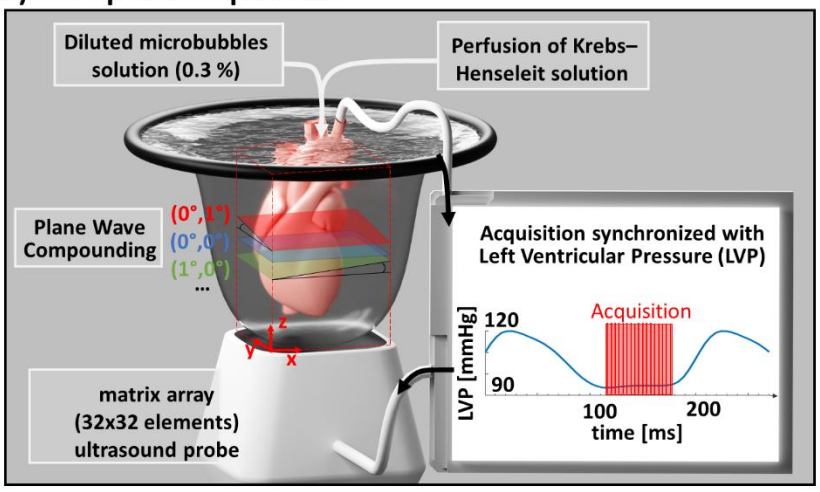

b) 3D Ultrasound Localization Microscopy

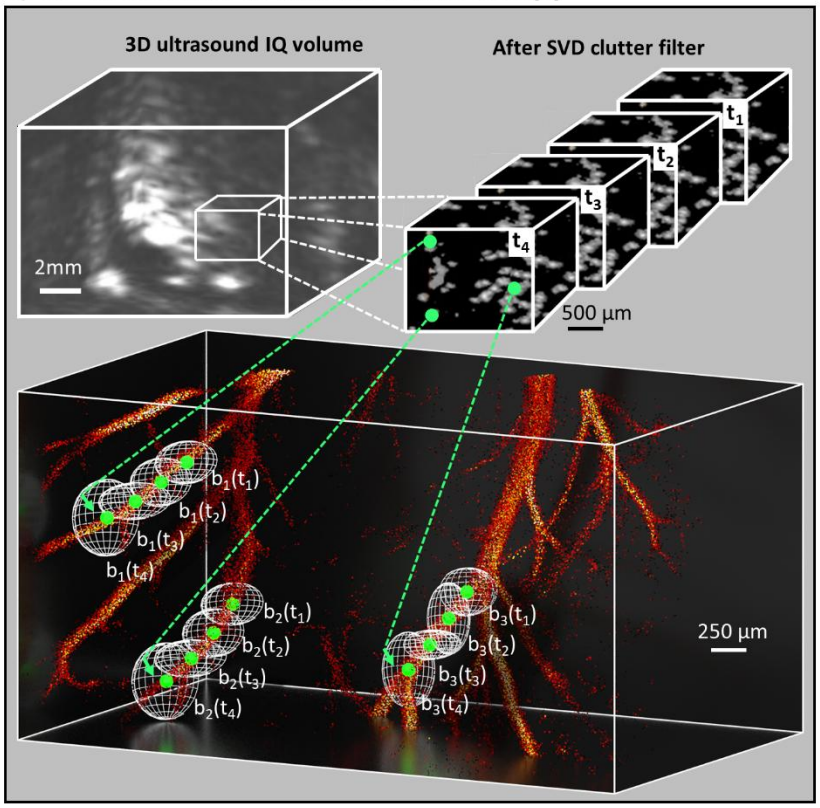

c) Multi scale motion correction

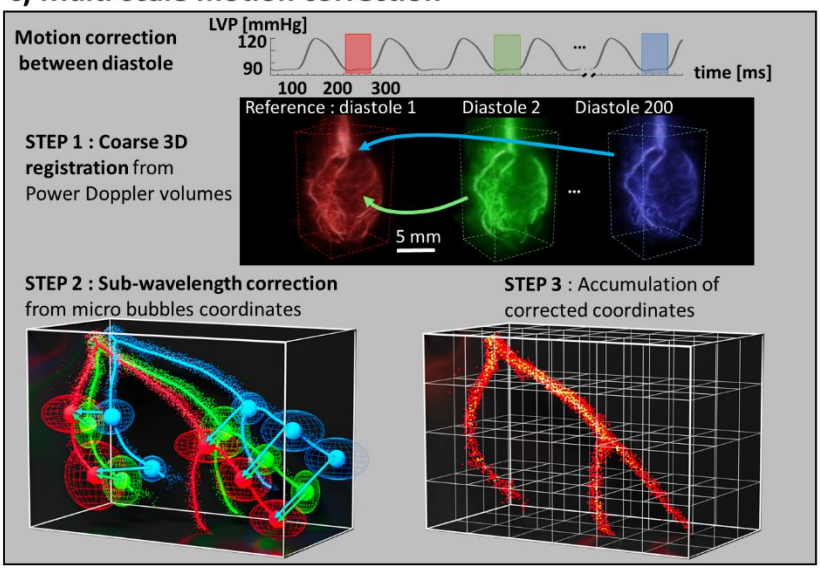

Figure 1. 3D CorULM principles: **a)** Langendorff set-up to study the perfused isolated beating rat heart with 3D ultrafast ultrasound imaging and Plane Wave Compounding (planes waves are depicted at different angles). The ultrasound acquisition is synchronized with LV Pressure. **b)** 3D Ultrasound Localization Microscopy is processed during diastolic phases: after SVD clutter filtering, contrast agent microbubbles (MB) are localized with a 3D paraboloid b_n and are tracked over acquisition times t_i to determine MB tracks. **c)** 3D intensity-based rigid registration is computed between Power Doppler volumes to correct potential motion between diastolic phases. Then, a second correction is computed at a subwavelength scale using an iterative closest point (ICP) algorithm to correct motion of the cloud of MB positions. Corrected coordinates are eventually used to create a 3D volume of the coronary flow.

In vivo imaging of rat coronary vasculature – Experimental model

Transthoracic *in vivo* imaging of 3 Sprague Dawley males of 208±2.3g were performed under 2% isoflurane gas anesthesia in 0.8 L/min 70% O2/30% air. Before positioning the matrix transducer, a conventional transthoracic echocardiography B-mode imaging was performed with a 12MHz linear array (Superlinear 20-6, Aixplorer, SuperSonic Imaging). Microbubbles were injected by insertion in the caudal vein of a 25 gauges catheter connected to a syringe positioned on a syringe withdraw. ECG and breathing were recorded by a data acquisition and analysis device (PowerLab-Labchart, ADintruments) using subcutaneously positioned electrodes for ECG and a spirometer connected to anesthesia face mask for breathing. Respiratory and ECG signals were computed in real-time to enable the acquisition of synchronized ultrafast imaging.

All animals received humane care in compliance with the European Communities Council Directive of 2010 (2010/63/EU), and the study was approved by the institutional and regional committees for animal care (Comité d'Ethique pour l'Expérimentation Animale no. 59 'Paris Centre et Sud', APAFIS#27733-2020101822261518 v2)

3D ultrafast ultrasound imaging

Isolated perfused hearts imaging: The hearts were immersed in the Krebs-Henseleit solution in a pool covered by a latex membrane. The ultrasound transducer was positioned in the apical view orientation and ultrasound gel was applied between the latex membrane and the

transducer (figure 1.a). The correct placement of the transducer was controlled using real-time biplane B-mode imaging.

A customized, programmable, 1024-channel ultrafast ultrasound system as described in Provost *et al*[10] and Papadacci et al 2020[13] was used to drive a 32-by-32 matrix-array probe centered at 9 MHz (60% bandwidth at 6dB). The system was composed of four research electronics (Vantage 256, Verasonics, Kirkland, WA, USA) which were assembled and synchronized, defining a single device containing 1024-channels in transmission and receive.

An ultrafast Doppler imaging sequence consisting of 9 plane waves defined by pair of angles (i,j) with i and j in (-5.7°, 0°, 5.7°) as depicted in (figure 1.a) was transmitted at a PRF of 20 kHz during 270ms. Backscattered echoes of cardiac tissues and circulating microbubbles were received by each element of the matrix transducer and the RF signals were stored in memories. Receive beamforming and coherent compounding[10] was performed on the RF data to obtain IQ demodulated volumes at an effective imaging rate of 2220 volumes/s. The high temporal volume rate is paramount for accurately quantifying the flow velocity. Volumes of $24 \times 13 \times 13$ mm^3 were reconstructed (depth and lateral directions respectively) with a voxel size of $0.862 \times 0.197 \times 0.197$ mm^3.

Blocks of ~100 frames (~50 ms) corresponding to the diastolic phase were then selected from both LVP signal and axial tissue velocity. This selection is described in more detail in the Supplemental Methods. This selection is described in more details in the supplementary materials. IQ data were then clutter-filtered using a spatio-temporal clutter filter (SVD) for each block[14] by removing the first 30 eigenvectors.

This sequence was repeated 100 times and each repetition was synchronized with the LVP signal and trigged with the beginning of the systolic phase.

In vivo imaging: The same imaging sequence (100 repetitions of 300ms blocks at a volume rate of 1333 Hz) and the same methods were used for the *in vivo* acquisition. In addition to

the ECG synchronization, a gating was performed on breathing pressure in order to trig the acquisition at the R peaks and when breathing pressure was low (end of exhalation). The rat heart rate was about 300 beats per minutes so that each block covered at least one complete cardiac cycle. A selection of 50 volumes (corresponding to 37 ms) was selected at the beginning of the diastole as shown in (figure 5.c).

2D ultrafast ultrasound imaging

2D imaging was exclusively used for imaging the non-beating isolated hearts. The hearts stopped beating by cooling the perfused solution down to 4°C. The probe was then placed in long axis view of the left ventricle. 2D imaging was performed using a linear probe (128 elements, 0.11 mm pitch, centered at 15.6 MHz) driven by a research electronics (Vantage 256, Verasonics, Kirkland, WA, USA) using 128 out of 256 channels in transmission and in receive.

The ultrafast imaging sequence consisted in 8 plane waves transmitted at angles [-7° -5° -3° -1° 1° 3° 5° 7°] at a PRF of 6400 Hz and a frame rate of 800 Hz during 625ms. This sequence was repeated 960 times giving a total accumulation time of 10 minutes. Signals received by the system were sampled at 60MHz and a 2D delay-and-sum beamforming with coherent compounding was performed to reconstruct the ultrasound frames at an effective frame rate of 800Hz. Images of $10 \times 14\,\mathrm{mm}^2$ were reconstructed (depth and lateral directions respectively) with a sampling of $0.1 \times 0.1\ \mathrm{mm}^2$ (~ the ultrasound wavelength).

3D Ultrasound Localization Microscopy processing and motion correction

The basic principle of 3D CorULM along with a lay-out of the approach used to image the hearts is depicted on Fig 1.a.b.c. In brief, 3D CorULM was based on several successive processing steps. The first step consisted in the 3D localization of single microbubbles at a subwavelength scale. Then, the microbubbles were tracked in 3D over successive frames to derive flow velocity. 3D motion correction was then applied between blocks of frames

associated to the different diastolic phases. CorULM maps are subsequently rendered by aggregating the corrected positions of the microbubbles flowing through the coronary network. All the processing steps are fully described in the supplementary materials.

Data processing was performed with MATLAB software (2020a, The MathWorks Inc., USA) using a 32-core 3 GHz AMD processor. Processing time was approximately 5 hours of beamforming and 4 hours of SVD filtering plus 3D Ultrasound Localization Microscopy processing for 100 blocks (corresponding to a total of 10,000 processed volumes).

Visualization and quantification

3D representations of CorULM results were computed using the volren function of Amira software (Amira v.6.0.1 software, Visualization Sciences Group, USA).

Diameter quantification through skeletonization

Automatic quantification of the vessel diameter was performed on the 3D CorULM density maps reconstructed with isotropic voxels of size 40 µm. A Gaussian filter was applied (σ = 40µm) and the skeletonization of the coronary vasculature was performed using the "auto-skeleton" function in Amira software. As a result of the skeletonization, the vessel diameters were quantified for every centerline point detected.

Flow rate quantification

The norm of the flow velocity was quantified at the centerline points of the skeleton and assumed to be the maximum velocity $Vmax$ of the velocity profile. Using the velocity and diameter measured previously, the flow rate was eventually computed assuming a Poiseuille flow: $Q = \pi r^2 \times \frac{Vmax}{2}$ (Q : flow rate, r: radius) for every detected vessel.

Functional quantification

To quantify the effect of vasodilation on microvascular vessels we computed the variation of vessel radius, flow velocity and flow rate in response to adenosine. Skeletons were extracted from acquisitions in baseline and under adenosine-induced vasodilation and spatially

registered the two skeletons using Coherent Point Drift registration[15]. After registration, vessels whose centerline points were closer than 150 µm were considered identical in the 2 acquisitions. We then performed several analyses of the flow and diameter variation for different classes of vessels.

In a first analysis, we quantified the radius, velocity, and flow rate in a class of microvascular vessels. We extracted all the vessels between 30 and 40 µm in radius at baseline, and computed the median value of radius, velocity, and flow rate in baseline and during adenosine infusion for each heart (N = 6).

In a second analysis, we investigated the vasodilation as a function of vessel size. We extracted vessels of different classes of radius (20-30; 30-40; 40-50; 50-60; >60 µm). For each vessel we computed its radius variation as the ratio of radius ($r_{adenosine}/r_{baseline}$) and quantified the median value per class and per heart.

In a third analysis, we computed the flow rate variation as the ratio ($q_{adenosine}/q_{baseline}$) for each vessel regardless of its size and compared the median value for each heart to the ratio of perfusion flow measured by the perfusion system during the same experiment. This control measurement was used as an estimate of the coronary flow reserve (CFR).

For 2D acquisitions, density and velocity maps were reconstructed with a pixel size of 5 x 5 μm^2. We analyzed the flow velocity profile across the section of a large vessel. The vessel cross-section was divided into 5 segments of the same length (26 µm). In each segment, we evaluated the velocity of individual flowing MBs assuming that each MB was an independent event.

AHA 17-segments representation

The 3D CorULM velocity map of the left ventricle was projected onto polar plot to provide the flow information on a 2D map. The standardized 17-segments model published by the American Heart Association (AHA)[16] was used to provide a regional representation and

determine the perfusion territories of the LV. The LV volume is segmented by manual delineation of the endocardial and epicardial borders on the ultrasound volumes. The LV volume is then separated into the 17 segments, a centerline of the LV (apex to base) is manually determined and a 2D polar plot is generated by projection of the maximal velocity in polar coordinates.

Micro Computed Tomography

After ultrasound imaging, hearts were perfused by adenosine 10^{-5} M for vasodilation followed by 10mL of 4% paraformaldehyde for fixation. Then, 2mL of microfil (Flow Tech, Carver, MA) was injected at a speed of 15mL/h. Microfil injection was optimized for complete casting of coronary arteries and veins without diffusion in the myocardium. Infusion was stopped when microfil started to flow out of the pulmonary vein. The heart with his perfusion set up were left until complete polymerization of the contrast agent (1h at room temperature)[17]. At the conclusion of the procedure, the hearts were immersed in 70% ethanol solution at 4°C for conservation.

Fixed hearts were imaged using an X- ray micro- CT device (Quantum FX Caliper, Life Sciences, Perkin Elmer, Waltham, MA). Full 3D high- resolution raw data were obtained by rotating both the x- ray source and the flat panel detector 360° around the sample (scanning time: 3 minutes). Views were reconstructed in stack of images containing 512 × 512 × 512 voxels (isotopic voxel size of 40 μm). The diameter of large coronary vessels was measured by CT and compared to corULM using Amira 3D visualization and analysis Software (Amira 6.0; Thermo Fischer Scientific USA). Right and left coronary arteries were segmented for both modalities (automatic segmentation tool) and the coronary diameters were measured with a 3D caliper.

Statistics

Spatial variations of velocity profiles were analyzed using unpaired 2-sided Student's *t*-test to evaluate the significance of difference at several locations of the flow profile assuming each MB event to be independent as explained in the Methods section. Linear regression was used on log-values to determine the exponent of the flow rate-radius relation. Median values of radius, velocity, and flow rate in baseline and under vasodilation were compared for each heart (N = 6) using a paired, 1-sided Student's *t*-test. Relative variations of radius were compared for several classes of vessels with a paired, 1-sided Student's *t*-test. Eventually, variations of flow rate were compared with the control measurements with a paired, 2-sided Student's *t*-test. For all box plots, center line (median), box (first and third quartiles), and whiskers, 1.5 × IQR with all data points, were individually plotted. Statistical significance was inferred for $P < 0.05$ with no significance (NS): $*P < 0.05$, $**P <$ 1e-2, $***P <$ 1e-3, $****P <$ 1e-4. Values are presented as mean ± SD unless specified.

Results

Coronary anatomy

CorULM provides high resolution images of the whole heart coronary vasculature as shown on Figure 2.a.i. When zooming at a smaller sale, the coronary microcirculation can be visualized as shown on Figure 2.a.iv. CorULM 3D images can be best visualized in a supplemental movie (Suppl. Video 1). Note that the spatial resolution in CorULM depends on the number of microbubbles passing through each reconstructed voxel and thus could potentially be improved by using longer acquisition time. Approximately 10 microbubbles are localized in each reconstructed voxel (20x20x20 μm^3) in the present result.

Quantification of the vessel diameter is performed automatically using a 3D center line extraction (skeletonization) algorithm. Diameters ranged from 20µm for tiny arterioles to ~300µm for larger branches of the right and left coronary arteries (Figure 2.a.v).

The coronary vasculature is compared to µCT performed on the fixed heart (Figure 2.a.viii). The vessel radius is quantified on 15 large vessels (134±35 µm) visualized in both modalities (supplementary figure 3) with a mean absolute error of 12µm between the two modalities. Gross photography of the fixed heart shows the overall anatomy of the rat heart (Figure 2.a.ix).

For comparison, CorULM is also performed in 2D on arrested hearts using high frequency imaging which is expected to provide higher resolution. Note that in 2D, CorULM cannot be performed on the beating hearts because of strong out of plane motion artefacts and requires the hearts to be arrested using low temperature liquid perfusion. The vasculature and flow velocity images of the left ventricular free wall are shown on Figure 2.b.i and Figure 2.b.ii. Vessels as small as 16µm are visible (Figure 2.b.iii). It was further possible to accurately assess the velocity profile across a relatively large vessel, revealing a Poiseuille like flow profile (Figure 2.b.iv).

Coronary flow assessment

The high temporal resolution of the 3D ultrafast imaging system further enables estimating the flow velocity via particle tracking (see methods section for a detailed description). Figure 2.a.ii shows the base to apex flow direction: downwards (in red) corresponding mainly to arterial flow and upwards (in blue) to veinous flow. Absolute flow velocity estimates range from 10mm/s in tiny arterioles up to more than 300 mm/s in large arteries (Figure 2.a.iii and 2.a.vi). Flow velocity can be better visualized in a supplemental movie (Suppl. Video 2). CorULM is compared to low-resolution power Doppler imaging (Figure 2.a.vii) obtained with the same IQ data[18]. Flow velocity were estimated as a function of perfusion pressure (supplementary figure 2).

The flow rate-radius relation is obtained on Figure 2.a.x for a large range of arterial radius [10-150 µm]. Fitting to a power law provides an exponent of 2.61 (r^2=0.96, p<0.001) which

is consistent with theoretical predictions and experimental validations of scaling laws in vascular trees, also known as the generalized extension of Murray's law[19].

Figure 2. Coronary Ultrasound Localization Microscopy

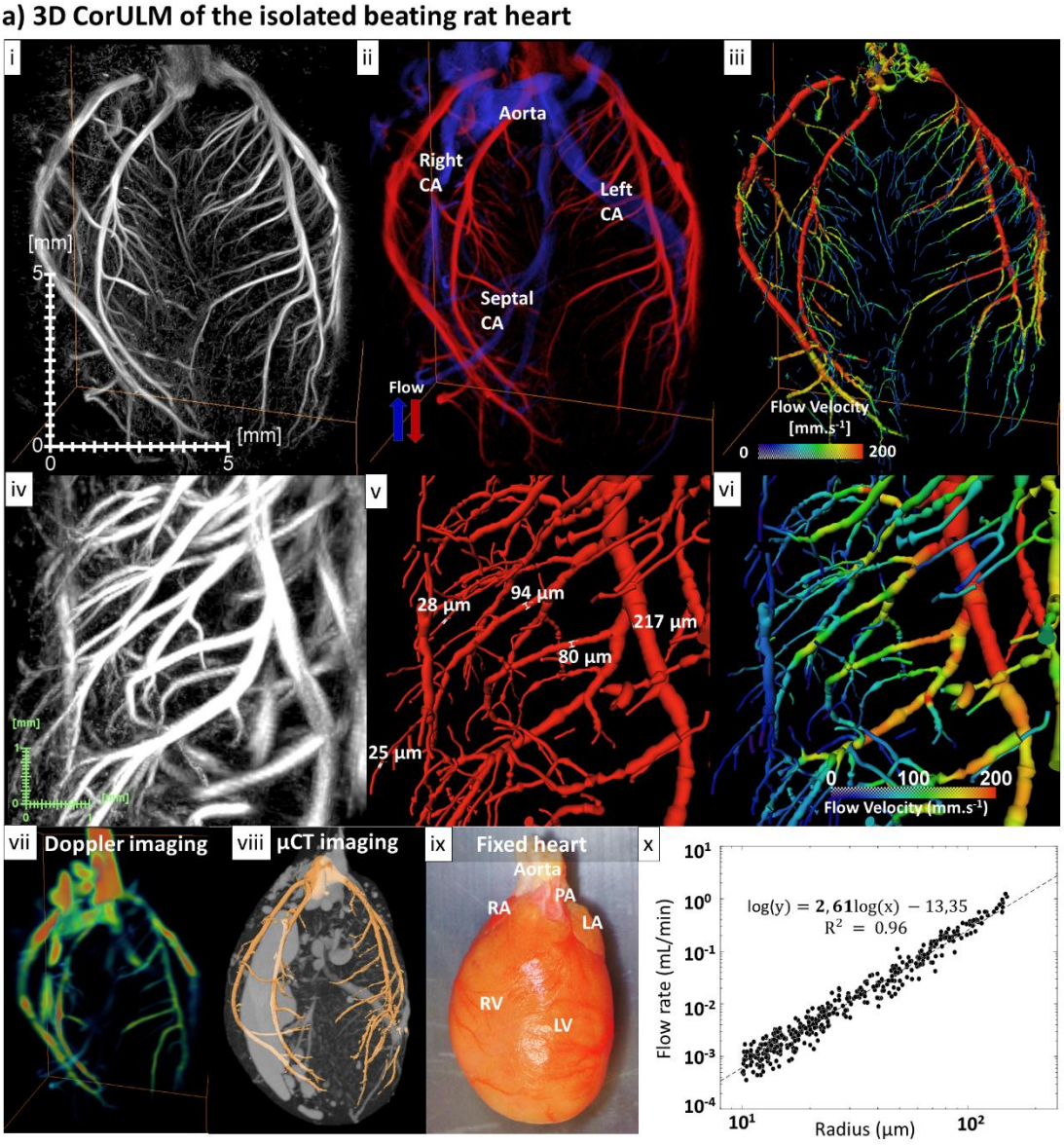

Figure 2. Coronary Ultrasound Localization Microscopy of isolated rat hearts: **a)** 3D CorULM is performed on a perfused beating rat heart to provide (i) 3D Density map, (ii) Directional flow velocity map which is used to identify the arterial (red) and venous (blue) flow and (iii) 3D flow velocity distribution. Micro-vessels are better visualized at a smaller scale on (iv) 3D density map of the microcirculation, (v) quantification of the micro-vessels diameter and (vi) velocity obtained from skeletonization. For comparison, the low-resolution Power Doppler map is shown on (vii) as well as µCT imaging (viii) and gross photography (ix) of the same fixed heart. (x) Analysis of flow rate as a function of radius in a large range of vessels reveals a power law with an exponent of 2.61. **b)** 2D CorULM density maps (i) and velocity (ii) are obtained in a non-beating rat heart (long axis view of the LV free wall). iii) A cross-section of several vessels (1,2 and 3 annotated in (i)) on the density map is performed to quantify the vessel diameters. iv) Analysis of the velocity profile in a large vessel (vessel 4 in (ii)) shows the variations of flow velocities across the vessel and the Poiseuille-like flow profile by unpaired two-sided Student's t-test.

We then investigated the flow variation in response to adenosine induced-vasodilation. Figure 3.a shows the overall increase of radius and blood velocity on the CorULM maps. Analysis of the velocity histograms reveals a shift of the velocity distribution in response to vasodilation (Figure 3.b). To analyze finely the changes of radius, flow velocity and flow rate (Figure 3.c) an ensemble of microvascular vessels (~100 segments of Ø 60-80 µm in each heart, N=6 hearts) is selected. The median radius, flow velocity and flow rate increase significantly with adenosine. We then analyze the vasodilation as a function of the vessel size and figure 3.d shows that the relative dilation in response to adenosine is much larger in small vessels: small vessels [20-30] µm are dilated by 1.57±0.26 whereas larger vessels (>60µm) changed only by 1.07±0.2 ($p<0.01$). The global flow rate is analyzed for the entire vasculature and a two-fold increase of the microvascular coronary flow rate is found in response to adenosine which is in good agreement with the overall perfusion flow rate (control measurement) that increased from 8.80 ± 1.03 mL/min to 16.54 ± 2.35 mL/min ($p<0.001$). This ratio known as the coronary flow reserve (CFR) provides an indirect functional assessment of the microcirculation which is used clinically. We show here that CorULM provides a local and direct quantification of the microvascular coronary flow variation (Figure 3.e).

Finally, the main Left Anterior Descending artery is ligated to induce a complete occlusion of the LAD. Figure 4.a shows the 3D reconstruction of the coronary vasculature and the disappearance of a large part of the LAD after occlusion. Projection of the blood flow velocity on the 17-segment model of the American Heart Association (AHA) enables a clear delineation of non-perfused territory (Figure 4.b).

Figure 3. Multi-scale coronary flow quantification

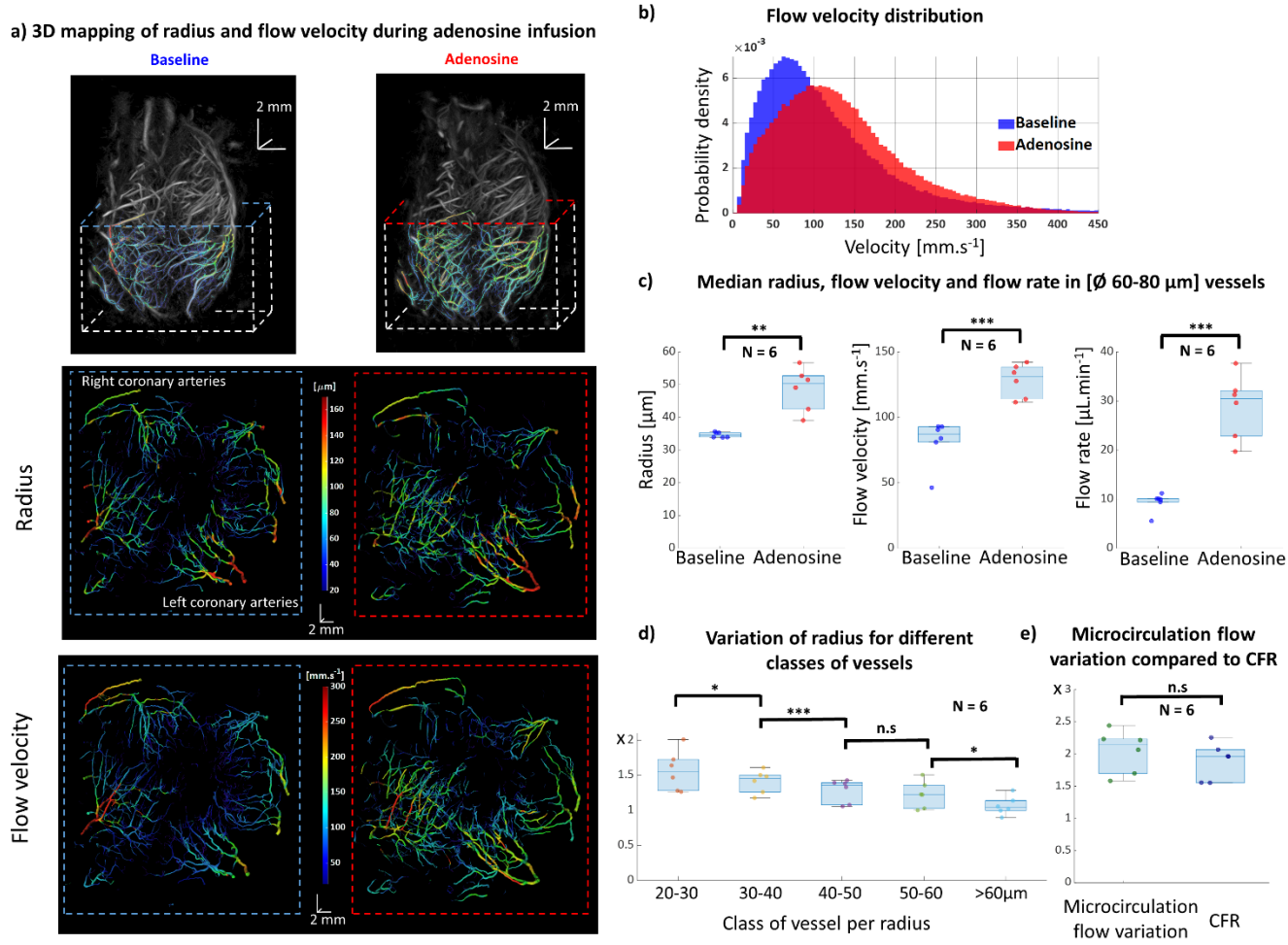

Figure 3. Multi-scale coronary flow quantification. a) Quantification of vessel radius and flow velocity in baseline (left side) and during adenosine-induced vasodilation (right side). Top panels: the flow velocity is overlaid on the density map (grayscale). Middle panels: 3D radius maps showing the increase of vessel radius with adenosine. Low panels: 3D flow velocity showing the velocity increase with adenosine. Middle and low panels correspond to top views of the white box region of interest shown in the top panels. **b)** The flow velocity distribution shows a shift towards higher velocities during adenosine-induced vasodilation. **c)** Radius, flow velocity and flow rate computed on an ensemble of microvascular vessels (135±90 segments of Ø 60-80 µm in each heart, N=6 hearts). Median radius, velocity and flow rate increase significantly with adenosine ($p<1E-2$). **d)** Relative variation of radius

before and after adenosine are analysed for different classes of vessels. The relative increase of radius is significantly higher in small vessels. **e)** The ratio of the flow rate with adenosine over baseline's is computed for microvascular vessels (427±250 segments of Ø 40-150 µm in each heart). The median of this ratio per heart is in good agreement with the control Coronary Flow Reserve (CFR) measured from the perfusion flow rate.
$n = 6$; paired, one sided paired-sample Student's t-test for c) and d), 2 sides paired-sample *t*-test for e).

Figure 4. Left Anterior Descending (LAD) Coronary occlusion

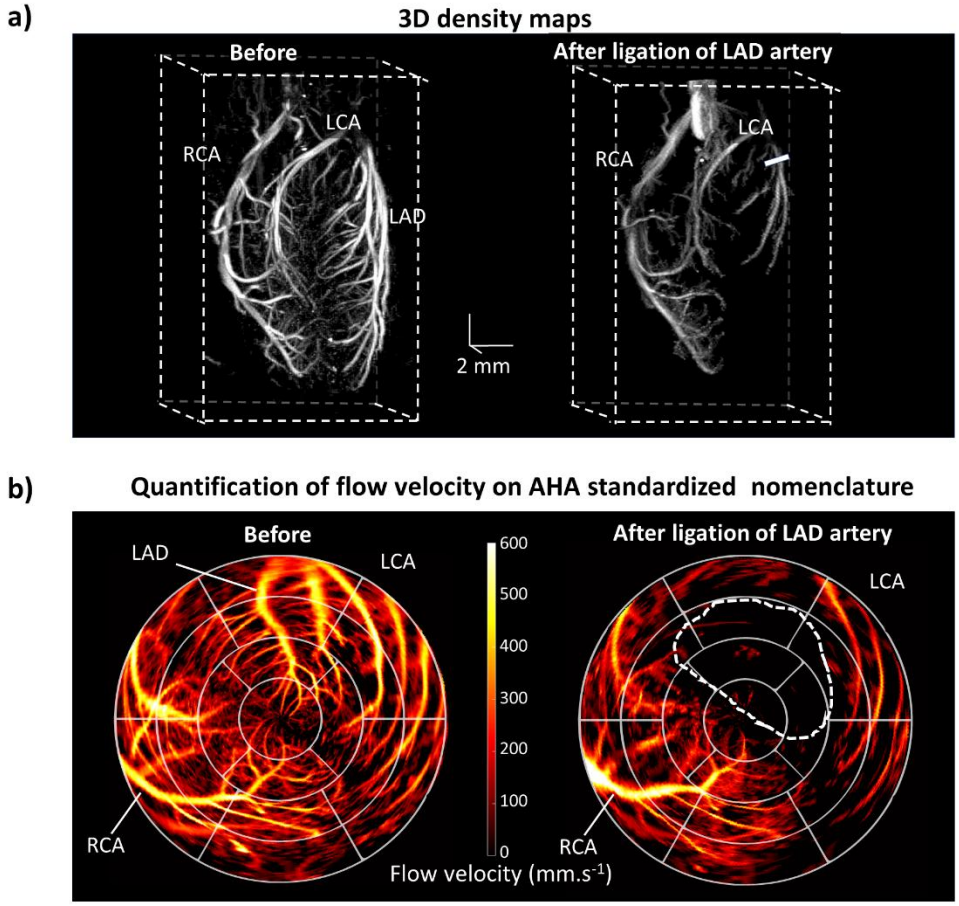

Figure 4. Left Anterior Descending (LAD) coronary occlusion. a) 3D density maps before and after Left Anterior Descending (LAD) coronary occlusion. Right Coronary Artery (RCA) and Left Circumflex Artery (LCA) are identified. b) The flow velocity is projected onto the bull's-eye AHA standardized representation of the left ventricle.

In vivo experiments

The feasibility of 3D CorULM was demonstrated in 3 closed chest rats. The matrix transducer was positioned on the rat chest (Figure 5.a) in parasternal view instead of the apical view because of ergonomic limitations due to the transducer dimensions. Figure 5.b shows that a large portion of the left ventricle can be reached with this orientation. One can notice however that several regions are shadowed by the ribs. In post-processing step, a short time window was determined in early diastole based on the analysis of the motion of the LV wall (Figure 5.c). The 3D Power Doppler map shows the coronary and left ventricular flow at low resolution (Figure 5.d.i). After 3D CorULM processing the coronary vessels are revealed at high resolution (Figure 5.d.ii). It should be noted that the microbubbles in the cavity are automatically removed by the tracking algorithm because the bubble concentration is too high. After vessel skeletonization, quantification of radius (Figure 5.d.iii) and flow velocity (Figure 5.d.iv) are performed and visualized. The radius of the vessels ranged from ~30µm for small arterioles to ~100µm for larger branches of the coronary arteries. Corresponding flow velocity estimates ranged from 10mm/s up to 300 mm/s with a negative gradient towards small branches.

Figure 5. *In vivo* imaging of the rat coronary vasculature

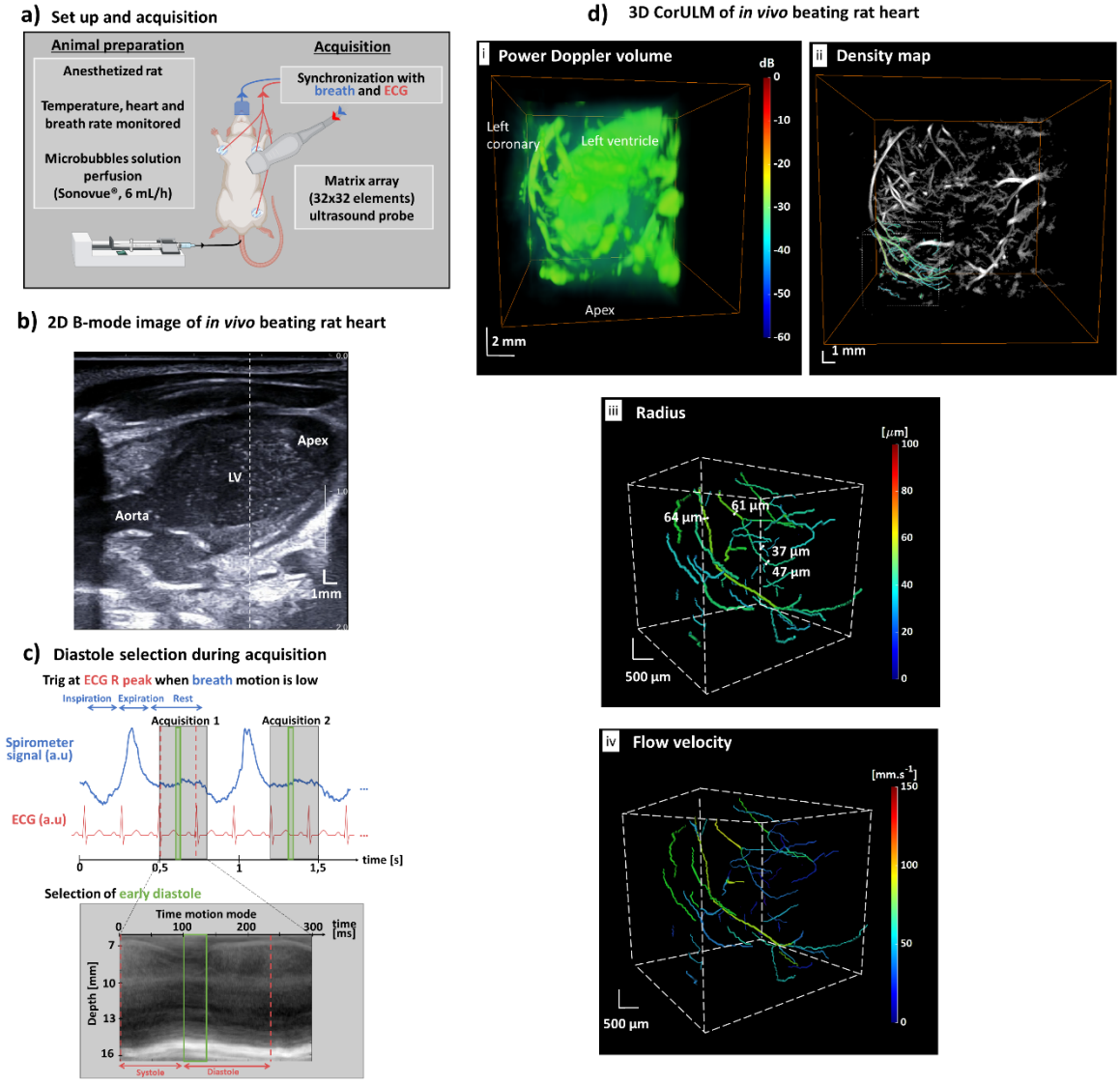

Figure 5. In vivo imaging of the rat coronary vasculature. a) *in vivo* acquisitions are performed using the matrix transducer positioned on the rat chest. The ultrasound acquisition is synchronized with ECG and breathing pressure. Microbubbles were injected into the caudal vein. Panel created with BioRender.com. **b)** A 2D B-Mode image shows the heart structures. **c)** A short time window of 37ms in early diastole is selected from the ultrasound data. **d)** The Power Doppler map shows the coronary and left ventricular flow at low resolution (i) whereas high resolution coronary vessels are revealed after 3D CorULM processing (ii). Radius are quantified inside the white box region and overlaid on the density map (grayscale). Micro-vessels are better visualized at a smaller scale with (iii) a quantification of the micro-vessels radius and (iv) velocity obtained from skeletonization.

Discussion

We hereby demonstrate that CorULM can visualize and quantify coronary microvascular flows in the beating hearts of rodents. The ability to image in 3D and subsequently to apply motion correction strategies empowers the recently developed ULM approach and enables imaging the microvascular flows in beating hearts. 3D ultrafast imaging is an important pre-requisite for successful application of CorULM as high-volume imaging rate (2200 volumes/s) is the key to correct 3D tissue motion and track successfully the microbubbles. Imaging of tiny coronary vessels <20µm in diameter was achieved across the whole heart (~20mm depth). Ultrafast imaging was previously used to image coronary vessels of about 100µm[20], we demonstrate here that CorULM can drastically improve the spatial resolution by one order of magnitude. Apart from its superb spatial resolution and mapping of the whole coronary vasculature with accurate diameter quantification, CorULM enables quantification of flow velocity and flow rate.

The flow rate increase in microvascular vessels is demonstrated and quantified after adenosine induced vasodilation. It allows the direct functional assessment of the microvascular coronary arterioles and is correlated to the coronary flow reserve. To our knowledge, it is the first imaging modality that can provide direct anatomical and functional visualization of coronary microvascular flow of the whole heart. The microvessels imaged by CorULM correspond to coronary arteries and arterioles (20 to 300 µm) which have a fundamental role in the metabolic regulation of coronary blood flow and are the site of regulation of flow resistance and thus cardiac perfusion.

In a broader perspective, CorULM can be used to facilitate early diagnosis based on biomarkers associated with microcirculatory alterations in cardiovascular disorders, while additionally providing new insights into disease progression, efficacy of drugs and other therapeutic interventions. CorULM should therefore strongly benefit to fundamental research

on coronary microvascular dysfunction and to the development of effective treatments. The setup of isolated retrograde perfused heart is commonly used as a preclinical model in cardiovascular research in physiology and drug developments and is particularly useful for the *ex vivo* investigation of ischemia-reperfusion injury. This *ex vivo* model has proved to be an irreplaceable and highly adaptable tool for research into coronary vascular function in physiological, pathological or pharmacological investigations, and into myocardium biochemistry and metabolism[21]. CorULM is particularly well adapted to isolated perfused heart of rats or mice as it provides the unique capability to visualize and quantify the microvascular flows of an entire heart with little modification of the Langendorff setup.

In vivo feasibility of transthoracic CorULM was then demonstrated on 3 rats. The acquisition system was slightly modified to take into account the respiratory motion. The potential of CorULM for the diagnosis of microvascular diseases will be further investigated on pathological animal models. In the long term, translation to the human heart could be achieved with lower frequency matrix transducers. 3D Ultrafast imaging of the human heart with a large field of view has been recently demonstrated using matrix transducers with diverging wave emissions[13,22,23] and could be applied to 3D CorULM.

Like any other cardiac imaging modalities, ultrasound micro-angiography has limitations. First, it requires acquisitions durations of a few tens of cardiac cycles (about 10s). Second, the current spatial resolution, estimated at 20x20x20 μm^3 could be improved by using matrix arrays with a refined one-wavelength spatial pitch leading to large angular aperture and smaller focal spots or by increasing frequency up to 15 MHz. The concentration and volume of sonovue used in this study should not be extrapolated directly to human applications. Further studies will be required to determine the optimal concentration and volume for coronary imaging application in large animals and human patients. Finally, we analyzed the blow flow only during the diastolic phase instead of the full cycle. In fact, there is also flow

during systole that could be identified during isovolumic systole and during late systole but the phasic blood flow pattern differs between large epicardial and penetrating coronary arteries. Indeed, mid-systole coronary blood flow velocity is retrograde in the intramyocardial arteries but antegrade in large epicardial arteries. Nevertheless, CorULM imaged small vessels where it is known that the majority of coronary blood velocity occurs during diastole[24]. Further technological and imaging development will allow to achieve full cycle analysis and thus taking into account the overall pattern of blood flow during the whole cardiac cycle.

3D ULM was applied to coronary mapping in this study but could be translated to any vascularized organs such as the brain or the liver. For instance, it could have a crucial impact on brain tumor applications to early detect angiogenesis responsible of recurrence after glioblastoma tumor resection.

Conclusion

We developed CorULM to image and quantify the microvascular coronary flow of beating hearts which provided unprecedented insights into the anatomy and function of coronary arteries. We anticipate that the advantages provided by CorULM will massively impact a large number of studies on clinically relevant coronary diseases and further foster the growing use of ultrafast ultrasound as a biomedical imaging tool.

Perspectives

Competency in Medical Knowledge

Patients with coronary microvascular disease have poor prognosis with significantly higher rates of cardiovascular events, including hospitalization for heart failure, sudden cardiac death, and myocardial infarction. Direct visualization of the full coronary architecture including complex microvascular network remains out of reach of current cardiac imaging modalities mainly due to inadequate temporal resolutions or sensitivity limitations. The results of this study show that direct and non-invasive imaging of the coronary microcirculation at the microscopic scale could be performed with ultrasound combined to microbubbles. It may offer a non-ionizing and portable technique for the visualization and quantification of microvascular flows.

Translational Outlook.

The major impact of this study is the development of 3D coronary ultrasound localization microscopy to visualize and quantify the coronary microcirculation on a beating heart. This technology is highly translational and has the potential to become a major tool for the clinical investigation of the coronary microcirculation.

References

1. Camici, P. G., d'Amati, G. & Rimoldi, O. Coronary microvascular dysfunction: mechanisms and functional assessment. *Nat Rev Cardiol* **12**, 48–62 (2015).
2. Gould, K. L. *et al.* Anatomic versus physiologic assessment of coronary artery disease. Role of coronary flow reserve, fractional flow reserve, and positron emission tomography imaging in revascularization decision-making. *J. Am. Coll. Cardiol.* **62**, 1639–1653 (2013).
3. Henningsson, M. *et al.* Diagnostic performance of image navigated coronary CMR angiography in patients with coronary artery disease. *J Cardiovasc Magn Reson* **19**, (2017).
4. Watanabe, N. *et al.* Noninvasive detection of total occlusion of the left anterior descending coronary artery with transthoracic Doppler echocardiography. *Journal of the American College of Cardiology* **38**, 1328–1332 (2001).
5. Fihn, S. D. *et al.* 2014 ACC/AHA/AATS/PCNA/SCAI/STS focused update of the guideline for the diagnosis and management of patients with stable ischemic heart disease: a report of the American College of Cardiology/American Heart Association Task Force on Practice Guidelines, and the American Association for Thoracic Surgery, Preventive Cardiovascular Nurses Association, Society for Cardiovascular Angiography and Interventions, and Society of Thoracic Surgeons. *J. Thorac. Cardiovasc. Surg.* **149**, e5-23 (2015).
6. Villemain, O. *et al.* Non-invasive imaging techniques to assess myocardial perfusion. *Expert Rev Med Devices* **17**, 1133–1144 (2020).
7. Errico, C. *et al.* Ultrafast ultrasound localization microscopy for deep super-resolution vascular imaging. *Nature* **527**, 499–502 (2015).

8. Couture, O., Hingot, V., Heiles, B., Muleki-Seya, P. & Tanter, M. Ultrasound Localization Microscopy and Super-Resolution: A State of the Art. *IEEE Transactions on Ultrasonics, Ferroelectrics, and Frequency Control* **65**, 1304–1320 (2018).
9. Cormier, P., Porée, J., Bourquin, C. & Provost, J. Dynamic Myocardial Ultrasound Localization Angiography. *IEEE Transactions on Medical Imaging* 1–1 (2021) doi:10.1109/TMI.2021.3086115.
10. Provost, J. *et al.* 3D ultrafast ultrasound imaging in vivo. *Phys Med Biol* **59**, L1–L13 (2014).
11. Heiles, B. *et al.* Ultrafast 3D Ultrasound Localization Microscopy using a 32×32 Matrix Array. *IEEE Trans Med Imaging* (2019) doi:10.1109/TMI.2018.2890358.
12. Abi-Gerges, A. *et al.* Decreased expression and activity of cAMP phosphodiesterases in cardiac hypertrophy and its impact on beta-adrenergic cAMP signals. *Circ Res* **105**, 784–792 (2009).
13. Papadacci, C., Finel, V., Villemain, O., Tanter, M. & Pernot, M. 4D Ultrafast Ultrasound Imaging of Naturally Occurring Shear Waves in the Human Heart. *IEEE Trans Med Imaging* **39**, 4436–4444 (2020).
14. Demené, C. *et al.* Spatiotemporal Clutter Filtering of Ultrafast Ultrasound Data Highly Increases Doppler and fUltrasound Sensitivity. *IEEE Trans Med Imaging* **34**, 2271–2285 (2015).
15. Myronenko, A. & Song, X. Point Set Registration: Coherent Point Drift. *IEEE Transactions on Pattern Analysis and Machine Intelligence* **32**, 2262–2275 (2010).
16. Standardized Myocardial Segmentation and Nomenclature for Tomographic Imaging of the Heart | Circulation. https://www.ahajournals.org/doi/full/10.1161/hc0402.102975.

17. Weyers, J. J., Carlson, D. D., Murry, C. E., Schwartz, S. M. & Mahoney, W. M. Retrograde perfusion and filling of mouse coronary vasculature as preparation for micro computed tomography imaging. *J Vis Exp* e3740 (2012) doi:10.3791/3740.

18. Correia, M. *et al.* Quantitative imaging of coronary flows using 3D ultrafast Doppler coronary angiography. *Phys. Med. Biol.* **65**, 105013 (2020).

19. Kassab, G. S. Scaling laws of vascular trees: of form and function. *American Journal of Physiology-Heart and Circulatory Physiology* **290**, H894–H903 (2006).

20. Maresca, D. *et al.* Noninvasive Imaging of the Coronary Vasculature Using Ultrafast Ultrasound. *JACC-Cardiovasc. Imag.* **11**, 798–808 (2018).

21. Skrzypiec-Spring, M., Grotthus, B., Szeląg, A. & Schulz, R. Isolated heart perfusion according to Langendorff—Still viable in the new millennium. *Journal of Pharmacological and Toxicological Methods* **55**, 113–126 (2007).

22. Papadacci, C. *et al.* 4D simultaneous tissue and blood flow Doppler imaging: revisiting cardiac Doppler index with single heart beat 4D ultrafast echocardiography. *Phys Med Biol* **64**, 085013 (2019).

23. Salles, S. *et al.* 3D Myocardial Mechanical Wave Measurements: Toward In Vivo 3D Myocardial Elasticity Mapping. *JACC Cardiovasc Imaging* **14**, 1495–1505 (2021).

24. Chilian, W. M. & Marcus, M. L. Phasic coronary blood flow velocity in intramural and epicardial coronary arteries. Circ Res 50, 775–781 (1982).

Supplementary Materials

3D Ultrasound Localization Microscopy processing

IQ volumes were first interpolated by two-fold in each dimension giving a voxel size of 0.05 x 0.1 x 0.1 mm^3 (depth and lateral directions respectively). Local maxima were then computed over the entire volume. Every local maximum neighborhood (kernel of size 11x11x11) was zero normalized and cross correlated with a Gaussian Point Spread Function (PSF) determined using Field II ultrasound simulations (σ_z = 0.4 σ_x = 0.9 and σ_y = 0.9 mm). Local maxima whose cross-correlation with PSF exceeded a given threshold (~0.65) and whose intensity value exceeded the 95th percentile of intensity distribution were labelled as micro bubbles.

Small volumes I(x,y,z) (3 x 3 x 3 voxels) centered on these selected local maxima were fitted with paraboloids of degree 2 of type $f(x,y,z) = a(x-x_o)^2 + b(y-y_o)^2 + c(z-z_o)^2$. MB center position were then defined as (x_o, y_o, z_o) for each fit.

MB center positions were stored over time to be tracked. We used an implementation of the Kuhn-Munkres algorithm or Hungarian method (https://github.com/tinevez/simpletracker, Jean-Yves Tinevez, 2021). For each particle of frame i, the square distance to all particles in frame i+1 was computed. The optimal pairing was given by minimizing the total square distance of matched particles. This algorithm was then looped in every frame. A maximum distance of 0.405 mm between two subsequent positions was allowed. Tracks smaller than 5 frames (~2 ms) were also rejected.

The tracks were then used to compute velocity measurement in three dimensions as explained in Heiles et al 2019[15]. Each particle had its instantaneous velocity computed as the ratio between its displacement vector and its temporal sampling $\frac{1}{volume\ Rate} = 0{,}45\ ms$. Traditional Lagrangian approach was used to calculate velocity fields.

Eventually, density maps were reconstructed from the MB center position. Providing a voxel size, the intensity value was given by the number of detected MB in this voxel. To avoid holes along a track, cumulated curvilinear abscissa was interpolated to create particles every 20 µm along each track. Similarly, velocity maps were reconstructed from the norm of velocity of every MB or one of their velocity components along the x, y or z axis, leading to quantitative and localized maps of coronary blood flow velocity.

The same algorithm was used for 2D and 3D imaging.

Motion correction

3D motion correction was applied between blocks of frames associated to different diastolic phases. A diastolic interval with low motion was defined as an interval with both, diastolic pressure and low axial motion. This interval was estimated for each heartbeat using the isovolumic LVP signal and the axial tissue velocity signal (Supplementary Figure 1.a). Diastolic pressure intervals were associated with intervals of constant LVP behavior applying a cut-off value on the differences between adjacent elements of the measured LVP signal. Tissue velocity was estimated by computing the axial velocity in the apex-aorta direction (v_z) from IQ demodulated beamformed volumes, using the Kasai estimator between successive non filtered IQ data. Low axial motion intervals were associated with intervals where the velocity was smaller than a predefined percentage of the maximum velocity (30 %), for each block.

A two-step rigid registration workflow was developed to correct for motion between blocks. A power Doppler image and MB tracked positions per block were used as inputs (Supplemental figure 1.b). The first registration step corrected for coarse motion. The intensity information in power Doppler images was used to compute the transformation that maximized the Advanced Normalized Correlation between a reference image and images

from other blocks. Power Doppler image associated with the block having the most tracked MB was selected as reference image. Output transformations were applied to MB tracked positions to correct for coarse motion. The second registration step corrected for sub-wavelength motion. An iterative closest point (ICP) algorithm was used to compute the transformation that minimized the Euclidean distance between the cloud of coarsely corrected MB positions tracked for each block and the cloud of MB positions of the reference block. Resulted ICP transformations were applied to obtain final (coarse + sub-wavelength) motion corrected MB positions. Power Doppler registration was implemented in Elastix 5.0 (https://elastix.lumc.nl/). ICP registration was implemented in MatLab R2020a. An example of motion correction of density maps for a representative case is shown in Supplemental figure 1.c.

For *in vivo* imaging, motion between each diastole selection was corrected as above. As the time selection of each diastole counts a few tens of ms, non-rigid motion was not corrected and assumed to be low.

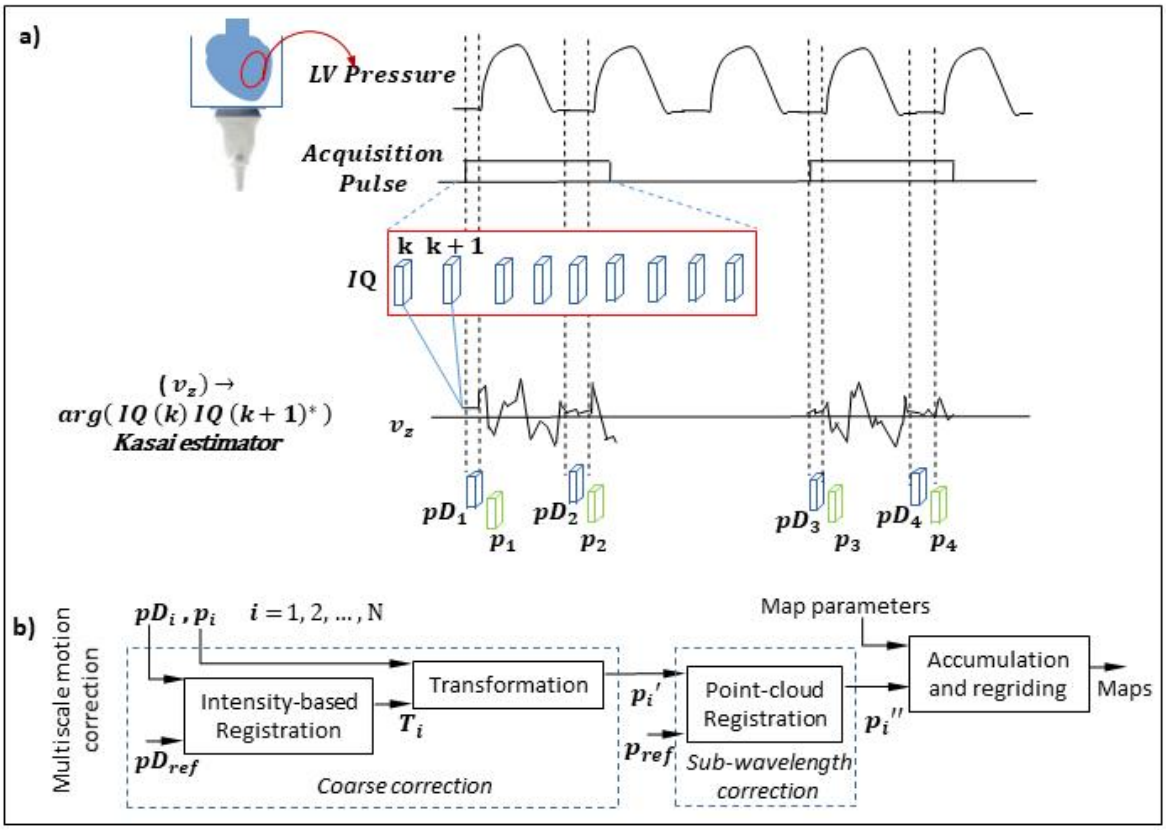
a)
LV Pressure
Acquisition Pulse
k k + 1
IQ
$(v_z) \rightarrow arg(IQ(k)\,IQ(k+1)^*)$
Kasai estimator
v_z
pD_1 pD_2 pD_3 pD_4
p_1 p_2 p_3 p_4
b)
Multiscale motion correction
$pD_i, p_i \quad i = 1, 2, \ldots, N$
Intensity-based Registration
Transformation
T_i
pD_{ref}
Coarse correction
p_i'
p_{ref}'
Point-cloud Registration
Sub-wavelength correction
Map parameters
Accumulation and regriding
p_i''
Maps

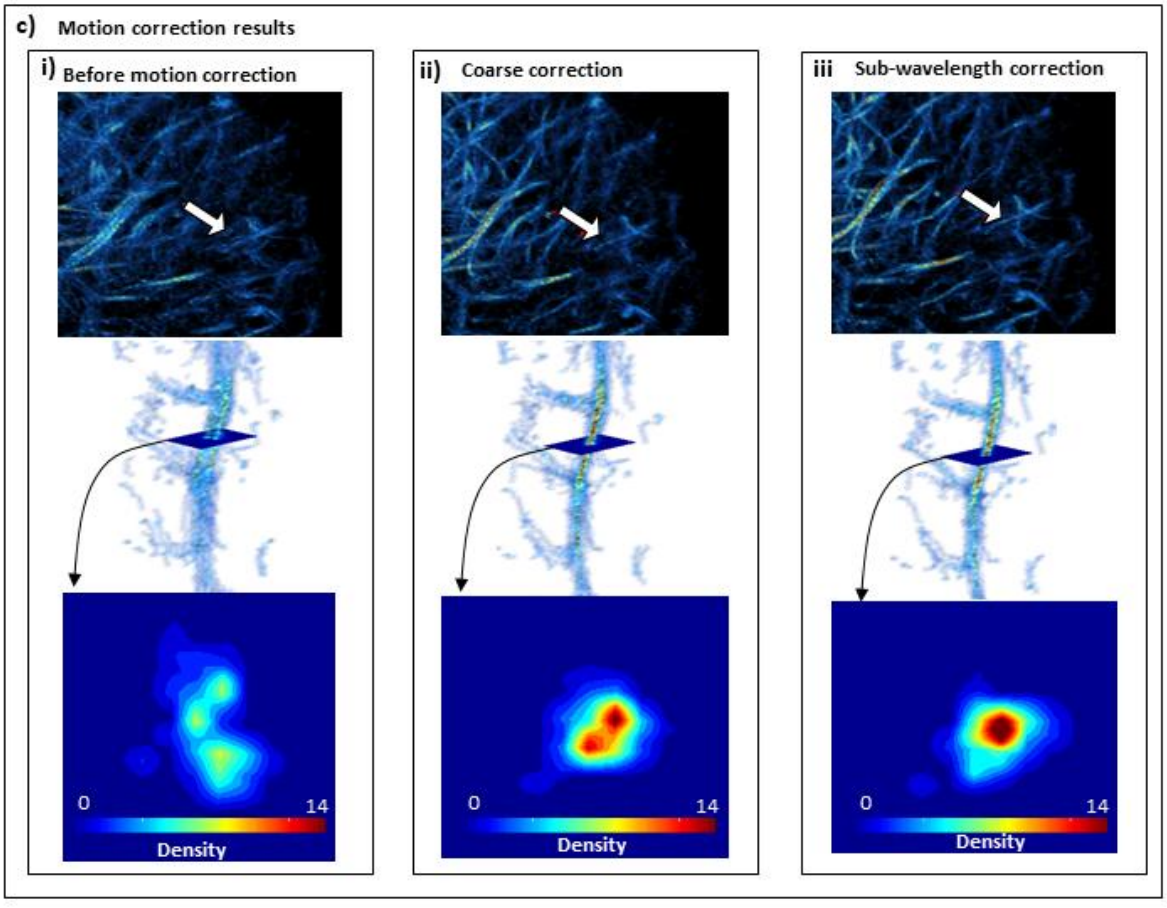
c) Motion correction results
i) Before motion correction
ii) Coarse correction
iii Sub-wavelength correction
0
14
Density

Supplementary figure 1: 3D registration and motion correction. a) Diastolic intervals are estimated using the left ventricle pressure (LVP) and the axial velocity in the apex-aorta direction (v_z). b) Multiscale motion correction workflow**:** the power Doppler image (pD_i) and tracked MB positions per block (p_i) are used as inputs for the 3D intensity-based registration and point cloud registration. c) Motion correction results: Density map before motion correction (i) after coarse correction (ii) and after sub-wavelength correction (iii). Detail of 3D density map (top), detail of isolated vessel showing the position of a transversal view (middle) and density values on transversal view (bottom). Same registration process is computed for *in vivo* data except in a) where diastole is extracted from a time-motion mode after a trig from breathing and ECG.

Response to perfusion pressure

N=3 isolated hearts, electrically stimulated at 350 bpm, were perfused by a Krebs-Henseleit solution for normal beating activity at constant coronary pressure at 60 and 120 mmHg. Coronary pressure was controlled by the perfusion heart system (see methods section for a detailed description). In each heart, radius and flow velocity were measured in 2 different vessels of similar size (Ø [220-440 µm]) at the two perfusion pressures to get flow rate variations assuming a Poiseuille flow. These variations are compared to the total perfusion flow rate variation when perfusion pressure increases and are presented in Supplementary

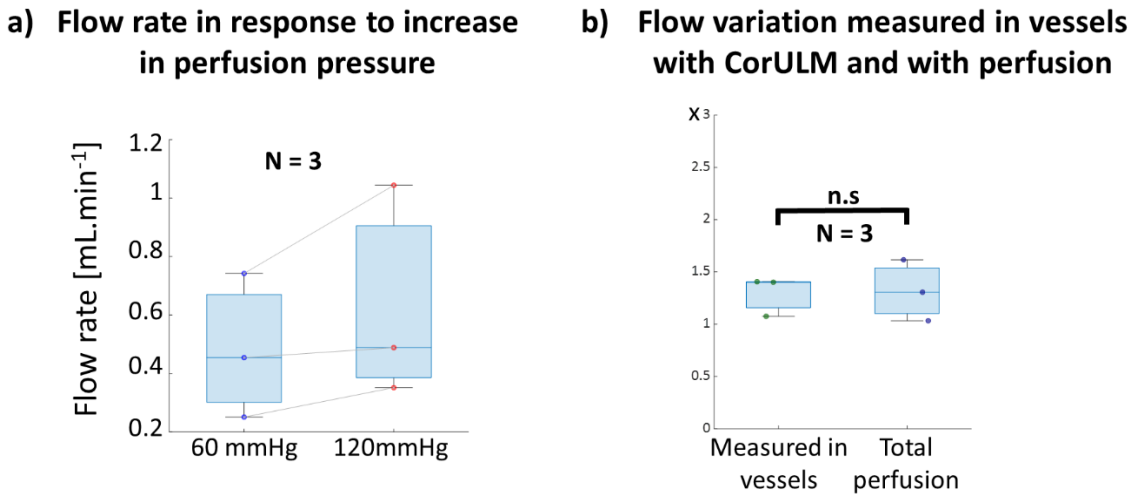

Figure 2.

Supplementary figure 2: flow velocity in response to changes in perfusion pressure **a)** For N=3 hearts under 2 perfusion pressures (60mmHg and 120mmHg), flow rates are computed on an ensemble of 2 vessels (Ø 220-240 µm in each heart). Individual data points are plotted above box plots and grey lines connect the pairs of observations. **b)** The ratio of the flow rate (perfusion at 120mmHg over perfusion at 60mmHg) is computed and is in good agreement with the one measured from the total perfusion flow rate variation. For all box plots: center

line, median; box, first and third quartiles; whiskers, 1.5× interquartile range (IQR) with all data points individually plotted (n = 3; n.s: non-significant, two sides paired-sample Student's t-test).

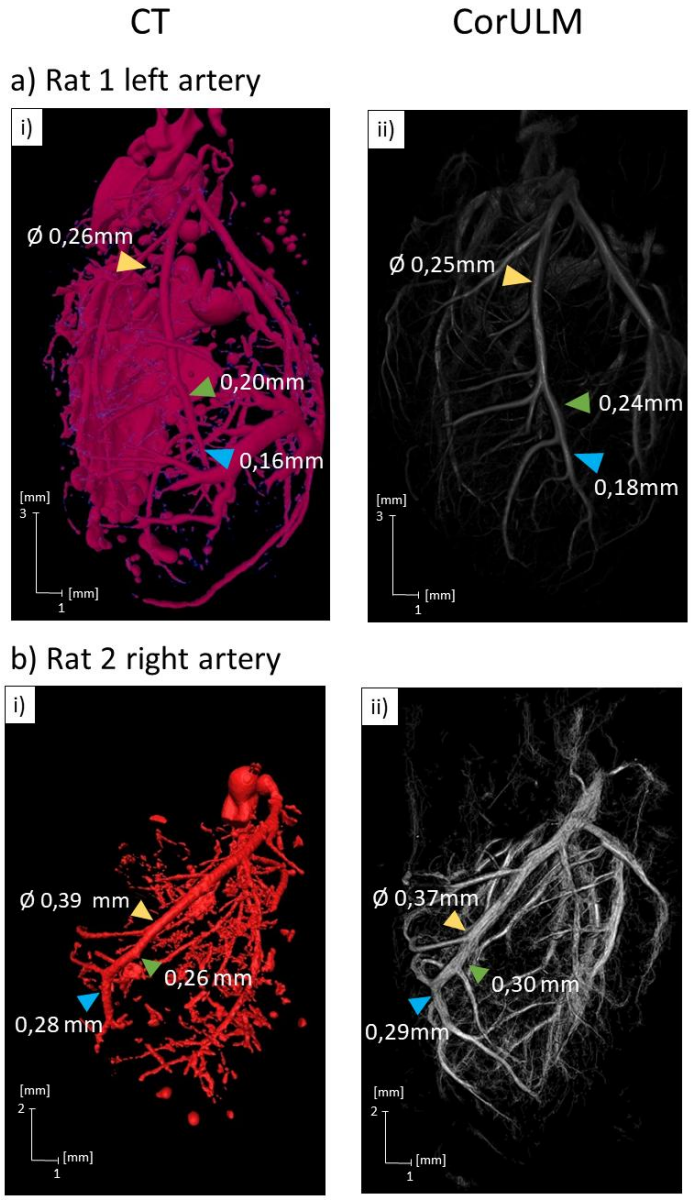

Supplementary figure 3: Comparison of µCT and CorULM on large coronary arteries. Coronary arteries segmented on Amira 6.0.1 software from CT acquisitions (left panels i) and from CorULM acquisitions (right panels ii). The vessels diameters are compared for a left coronary artery (a) and a right coronary artery from another rat (b).

Supplementary video 1: 3D CorULM rendering: Volume rendering of the CorULM density map obtained on a perfused beating heart.

Supplementary video 2: 3D flow rendering: Volume rendering of the 3D coronary flow velocity reconstruction obtained on a perfused beating heart.